

Determination of Carbon-13 Chemical Shielding Tensor in the Liquid State by Combining NMR Relaxation Experiments and Quantum Chemical Calculations

O. Walker, P. Mutzenhardt,* P. Tekely, and D. Canet

Contribution from the Laboratoire de Méthodologie RMN, ESA CNRS 7042,
INCM-FR CNRS 1742, Université H. Poincaré, Nancy I, B.P. 239,
54506 Vandoeuvre-lès-Nancy Cedex, France

Received July 20, 2001

Abstract: Based on multifield NMR relaxation measurements and quantum chemistry calculations, a strategy aiming at the determination of the chemical shielding tensor (CST) in the liquid state is described. Brownian motions in the liquid state restrict the direct observation of CST to a third of its trace (isotropic shift), and even if CST can be probed indirectly through some spin relaxation rates (specific longitudinal relaxation rates, dipolar chemical shift anisotropy (CSA) cross-correlation rates), an insufficient number of experimental parameters prevents its complete determination. This lack of information can be compensated by using quantum chemical calculations so as to obtain the molecular CST orientation even if a relatively modest level of computation is used. As relaxation parameters involve a dynamic part, a prerequisite is the determination of the molecular anisotropic reorientation which can be obtained independently from dipolar cross-relaxation rates. A polycyclic molecule exhibiting a well-characterized anisotropic reorientation serves as an example for such a study, and some (but not all) carbon-13 chemical shielding tensors can be accurately determined. A comparison with solid-state NMR data and numerous chemical quantum calculations are presented.

Introduction

Solid-state NMR is certainly the most adequate technique for measuring chemical shift tensors (CST).¹ Principal components of CST appear directly in the corresponding spectra, and the possible overlap of chemical shift anisotropy patterns is efficiently solved by using multidimensional techniques.² Thus, the resulting principal components can be measured with a satisfactory accuracy. Another way consists of dissolving the target compound in an oriented medium,³ making possible the determination of both the orientation and the magnitude of the CST, with the requirement of determining the molecule's orientation beforehand. This procedure has been recently applied to labeled proteins dissolved in bicelles for accessing proton, nitrogen, and carbon CST.⁴ The situation in the liquid state is by far more difficult, the rapid reorientation motion of molecules reducing the direct observation of the CST to a third of its trace (isotropic chemical shift); the only way of obtaining information about CST is based on spin relaxation measurements. Determination of CST in the liquid state is desirable for polycyclic compounds since significant modification between the liquid and the solid states can be expected from changes of the

electronic distribution around the relevant nuclei.⁵ The CST can also be modified or partly averaged by the presence of rapid internal motions, as is certainly the case in flexible and large molecules such as proteins.⁶ The scope of this paper is to devise such a strategy in the context of medium-size polycyclic molecules regardless of their dynamical properties and of the shielding tensor nature. In other words, the problem will be treated in the case of a fully anisotropic molecular reorientation and without considering any particular symmetry of the CST.

The first stage of our approach is the determination of the rotational diffusion tensor of the molecule. This is mandatory, as all NMR relaxation rates depend (i) on dynamical properties, (ii) on structural parameters (interatomic distances and angles), and (iii) possibly on chemical shift anisotropy. To characterize unambiguously molecular reorientation, only dipolar (¹H-¹³C) cross-relaxation rates, obviously independent of any contribution of chemical shift anisotropy, were used.⁷ In a second stage, all available NMR relaxation rates involving contributions from CST were measured (some of them at different values of the magnetic field) and finally combined with tensor orientations (obtained through quantum chemical calculations) so as to extract the shielding principal components of carbon-13 directly bound to proton(s).

* To whom correspondence should be addressed. E-mail: Pierre.Mutzenhardt@rmn.uhp-nancy.fr.

- (1) Grant, D. M. In *Encyclopedia of Nuclear Magnetic Resonance*; Grant, D. M., Harris, R. K., Eds.; John Wiley & Sons Ltd.: Chichester, 1996; Vol. 2, pp 1298–1321.
- (2) Barich, D. H.; Orendt, A. M.; Pugmire, R. J.; Grant, D. M. *J. Am. Chem. Soc.* **2000**, *124*, 8290–8295.
- (3) Lounila, J.; Jokisaari, J. *Prog. NMR Spectrosc.* **1982**, *15*, 249–290.
- (4) Comilescu, G.; Bax, Ad. *J. Am. Chem. Soc.* **2000**, *122*, 10143–10154.

- (5) Guenneau, F.; Mutzenhardt, P.; Assfeld, X.; Canet, D. *J. Phys. Chem. A* **1998**, *102*, 7199–7205.
- (6) Scheurer, C.; Skrynnikov, N. R.; Lienin, S. F.; Straus, S. K.; Brüschweiler, R.; Ernst R. R. *J. Am. Chem. Soc.* **1999**, *121*, 4242–4251.
- (7) Mutzenhardt, P.; Walker, O.; Canet, D.; Haloui, E.; Furo, I. *Mol. Phys.* **1998**, *94*, 565–569.

Theory

Chemical shielding is a tensorial quantity which can be expressed in the molecular frame according to

$$\sigma = \begin{bmatrix} \sigma_{XX} & \sigma_{XY} & \sigma_{XZ} \\ \sigma_{YX} & \sigma_{YY} & \sigma_{YZ} \\ \sigma_{ZX} & \sigma_{ZY} & \sigma_{ZZ} \end{bmatrix} \quad (1)$$

As, in the context of this study, only its symmetric part will be active,⁸ σ can be decomposed into a traceless antisymmetric tensor and a symmetric tensor:^{9,10}

$$\sigma = \sigma^{\text{sym}} + \sigma^{\text{anti}} \quad (2)$$

where

$$\sigma^{\text{sym}} = \frac{(\sigma + \sigma^T)}{2} \quad \text{and} \quad \sigma^{\text{anti}} = \frac{(\sigma - \sigma^T)}{2}$$

(σ^T stands for the transposed matrix). σ^{sym} can be transformed into its specific principal axis system (PAS), where the CST is expressed in terms of three principal components defined in ascending order (such as $\sigma_{xx} \leq \sigma_{yy} \leq \sigma_{zz}$):

$$\sigma^{\text{sym}} \rightarrow \sigma_{\text{d}}^{\text{sym}} = \begin{bmatrix} \sigma_{xx} & 0 & 0 \\ 0 & \sigma_{yy} & 0 \\ 0 & 0 & \sigma_{zz} \end{bmatrix} \quad (3)$$

The tensor is generally characterized by its anisotropy $\Delta\sigma$ and its asymmetry η , defined as

$$\Delta\sigma = \sigma_{zz} - (\sigma_{xx} + \sigma_{yy})/2 \quad (4)$$

$$\eta = (3/2)(\sigma_{yy} - \sigma_{xx})/\Delta\sigma \quad (5)$$

Usually, the three principal components, as well as the orientation of the PAS, are measured from solid-state NMR experiments. In the liquid state, because of Brownian motions, the sole and directly observable quantity is the isotropic chemical shift, $\delta_{\text{iso}} = \sigma_{\text{iso}}^{\text{ref}} - \sigma_{\text{iso}}$ (where $\sigma_{\text{iso}} = (1/3)(\sigma_{xx} + \sigma_{yy} + \sigma_{zz})$) and $\sigma_{\text{iso}}^{\text{ref}}$ is the isotropic chemical shift of a reference compound). For further information on CST in the liquid state, we must turn toward relaxation and, more specifically, toward the longitudinal relaxation and cross-correlation relaxation rates. Although expressions of relaxation rates involving an axial tensor ($\sigma_{xx} = \sigma_{yy}$, $\eta = 0$) are well known and of routine use, corresponding expressions for tensors without axial symmetry are less common and may be worth being recalled. A convenient procedure consists of decomposing a given tensor T into two axially symmetric tensors¹¹ with respect to z and x ; this yields

$$T = T'_z + T'_x \quad (6)$$

In this way, eq 3 becomes

$$\sigma_{\text{d}}^{\text{sym}} = \sigma'_z + \sigma'_x \quad (7)$$

which implies the definition of two anisotropies, $\Delta\sigma_z = (\sigma_{zz} - \sigma_{yy})$ and $\Delta\sigma_x = (\sigma_{xx} - \sigma_{yy})$. Now, because spectral densities

involved in any relaxation rate are the Fourier transform of a (auto- or cross-) correlation function,¹² the spectral density corresponding to an autocorrelation function J^T can be expressed as

$$J^T = J^{T'_z} + J^{T'_x} + 2J^{T'_z, T'_x} \quad (8)$$

where $J^{T'_z, T'_x}$ is a cross-correlation spectral density. In a general way, when dealing with well-defined relaxation vectors or axes, each spectral density can be written as

$$J^{r, r'}(\omega) = K^r K^{r'} \tilde{J}^{r, r'}(\omega) \quad (9)$$

K is a scaling factor, depending on the considered relaxation mechanism. In the case of the dipolar interaction between two nuclei A and X, r_{AX} being the internuclear distance,

$$K^{d(\text{AX})} = \sqrt{\frac{3\mu_0}{54\pi}} \frac{\gamma_A \gamma_X}{r_{\text{AX}}^3} \quad (10)$$

whereas for the so-called chemical shift anisotropy (CSA) mechanism, one has, in the case of an axially symmetric tensor,

$$K^{\text{CSA}} = -\sqrt{\frac{2}{45}} \Delta\sigma \gamma B_0 \quad (11)$$

Finally, the reduced spectral densities $\tilde{J}^{r, r'}$ depend on the angle between the relaxation vectors characteristics of mechanisms r and r' . In our case and according to eqs 8, 9, and 11, the CSA contribution to the longitudinal relaxation rate of a carbon-13 (denoted as C in the following) can be written as

$$R_1^{\text{CSA(C)}} = \frac{1}{15} \gamma_C^2 B_0^2 [(\Delta\sigma_z)^2 \tilde{J}^{\text{CSA(z)}}(\omega_C) + (\Delta\sigma_x)^2 \tilde{J}^{\text{CSA(x)}}(\omega_C) + 2\Delta\sigma_x \Delta\sigma_z \tilde{J}^{\text{CSA(z), CSA(x)}}(\omega_C)] \quad (12)$$

(when $r = r'$, $\tilde{J}^{r, r'}$ has been noted \tilde{J}^r). In eq 12, the reduced spectral densities refer to the x and z directions of the shielding tensor principal axis system and must be specified with respect to the rotational diffusion tensor. Their expressions can be derived from Hubbard's paper¹³ and are given in the Supporting Information. Next, the simplifying assumption of an isolated ¹³C–H spin pair will be considered. A detailed description of the interference effects on the relaxation of two unlike spins ^{1/2} has been presented by Goldman,¹⁴ and therefore his treatment will be only briefly summarized. In the presence of cross terms between the chemical shift anisotropy relaxation mechanism of a carbon-13, denoted by CSA(C), and the dipole–dipole relaxation mechanism between this carbon and a proton (usually the proton directly bonded to this carbon), denoted by $d(\text{H–C})$, the two components of the carbon doublet relax at different rates (implying that a sufficiently large J coupling constant exists between the two considered nuclei that one is able to probe the behavior of each line within the considered doublet). Their transverse relaxation rates R_2^α and R_2^β can be expressed as $R_2^\alpha = R_2 + \sigma^{d(\text{H–C}), \text{CSA(C)}}$ and $R_2^\beta = R_2 - \sigma^{d(\text{H–C}), \text{CSA(C)}}$. R_2 is the classical transverse relaxation rate, whereas $\sigma^{d(\text{H–C}), \text{CSA(C)}}$ refers to the CSA(C)– $d(\text{H–C})$ cross-correlation rate arising from the

(8) Kowalewski, J.; Werbelow, L. *J. Magn. Reson.* **1997**, *128*, 144–148.
 (9) Anet, F. A. L.; O'Leary, D. J. *Concepts Magn. Reson.* **1991**, *3*, 193–214.
 (10) Mason, J. *Solid. State. Nucl. Magn. Reson.* **1993**, *2*, 285–288.
 (11) Werbelow, L. *Nuclear Magnetic Resonance Probes of Molecular Dynamics*; Kluwer Academic: Dordrecht, 1994; Chapter 5.

(12) Details of calculations can be found in the following: Canet, D. *Concepts Magn. Reson.* **1998**, *10*, 291–297.
 (13) Hubbard, P. S. *J. Chem. Phys.* **1970**, *52*, 563.
 (14) Goldman, M. *J. Magn. Reson.* **1984**, *60*, 437–452.

interference between these two relaxation mechanisms. Subtracting the two relaxation rates provides the cross-correlation term, which can be expressed as

$$\sigma^{d(\text{H-C}),\text{CSA}(\text{C})} = \frac{1}{2} \sqrt{\frac{3}{2}} \tilde{J}^{d(\text{H-C}),\text{CSA}(\text{C})}(\omega_{\text{C}}) + \sqrt{\frac{2}{3}} \tilde{J}^{d(\text{H-C}),\text{CSA}(\text{C})}(0) \quad (13)$$

Using previous developments and notations, this yields

$$\sigma^{d(\text{H-C}),\text{CSA}(\text{C})} = -\frac{\mu_0 \gamma_{\text{H}} \gamma_{\text{C}}^2 B_0 \hbar}{4\pi r_{\text{CH}}^3} \left[\frac{1}{10} (\Delta\sigma_z \tilde{J}^{d(\text{H-C}),\text{CSA}(z)}(\omega_{\text{C}}) + \Delta\sigma_x \tilde{J}^{d(\text{H-C}),\text{CSA}(x)}(\omega_{\text{C}})) + \frac{2}{15} (\Delta\sigma_z \tilde{J}^{d(\text{H-C}),\text{CSA}(z)}(0) + \Delta\sigma_x \tilde{J}^{d(\text{H-C}),\text{CSA}(x)}(0)) \right] \quad (14)$$

Other relaxation rates can be envisaged. The transverse relaxation rate R_2 possesses also a contribution arising from the CSA mechanism. Unfortunately, an accurate measurement of its absolute value in small or medium-size molecules proved to be difficult. The main reason is the smallness of R_2 , implying the application of a long CPMG¹⁵ pulse train prone to pulse imperfections and sample temperature variations. Other candidates could be the CSA–CSA interference terms,¹⁶ but with a nonlabeled compound it seems illusory to measure such interaction between two carbons-13. On the other hand, measurement of the CSA(^1H)–CSA(^{13}C) cross-correlation rate turned out to be unrealistic because of the weakness of the proton CSA. At the outcome, for each carbon-13 in the molecule, three independent experimental parameters depending on CST appear reliable: (i) the isotropic chemical shift, (ii) the CSA contribution to the longitudinal relaxation rate, and (iii) the cross-correlation term between the CSA and the dipolar mechanism.

Now, the first point to address is how to characterize the molecular tumbling without resorting to these three parameters. This can be achieved by the extensive use of ^1H – ^{13}C cross-relaxation rates. Indeed, a fully anisotropic reorientation is totally described if at least six different cross-relaxation rates belonging to six non-collinear ^1H – ^{13}C vectors are available in the molecule (this number is reduced to three if it can be postulated that the rotational diffusion tensor and the inertial tensor are identical). These cross-relaxation rates, independent of CST, can be written as

$$\sigma^{d(\text{H-C})} = (K^{d(\text{H-C})})^2 [6\tilde{J}^{d(\text{H-C})}(\omega_{\text{H}} + \omega_{\text{C}}) - \tilde{J}^{d(\text{H-C})}(\omega_{\text{H}} - \omega_{\text{C}})] \quad (15)$$

Starting with an experimental or a theoretical geometry for the molecule, the orientation of the diffusion tensor is first assumed to be identical to the inertial molecular tensor. By modifying the relative orientation of the diffusion tensor with respect to the inertial tensor, one can search for the relative orientation which minimizes the difference between calculated and experimental cross-relaxation rates. In actual practice, all possible relative orientations are considered, and, for each orientation, the three correlation times characterizing a fully anisotropic

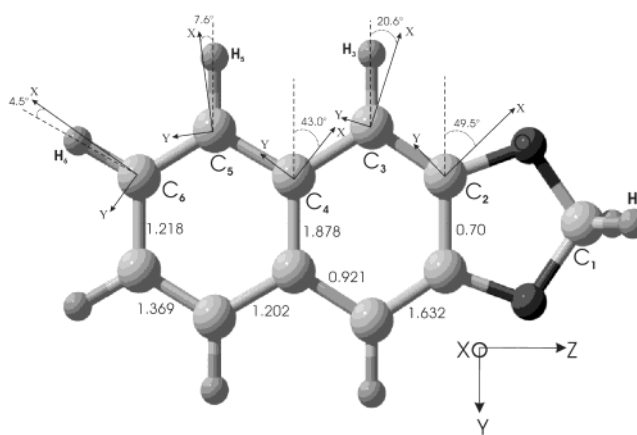


Figure 1. 2,3-Naphtho-1,3-dioxol molecule. X, Y, and Z refer to the rotation diffusion PAS (assumed to coincide with the inertial one). The z direction of chemical shift tensors is perpendicular to the molecular plane. The x and y directions of this tensor are shown by arrows at the location of each carbon. CST orientations and Mayer bond order were calculated at the GIAO-B3PW91/6-311++G** level of theory.

reorientation are optimized.¹⁷ At the outcome, the orientation corresponding to the smallest deviation will be retained.

At this point, if no hypothesis can be made about the magnitude and the orientation of carbon CST, only three relevant experimental measurements are available to determine six parameters (the three principal components of the CST and the three angles which define its orientation). This drawback can be circumvented by mixing NMR relaxation measurements with CST derived from a quantum chemistry approach. For the past few years, calculation of nuclear magnetic shielding constants has become an increasingly popular area for quantum chemical applications.¹⁸ From the several contributions to this topic, one can elaborate a strategy to obtain quite accurate results (with an accuracy of some parts per million). In fact, it will be shown in the quantum chemistry section that it is not necessary to run state-of-the-art calculations to extract the relative tensor orientation (which is indeed the information required to interpret relaxation data).

Experimental Section

The 2,3-naphtho-1,3-dioxol compound (Figure 1), dubbed ND11, was synthesized by Dr. J. P. Joly.¹⁹ This compound was chosen for several reasons: (i) it is essentially planar and sufficiently rigid that we can expect a strong anisotropy of its reorientation, (ii) carbons within aromatic rings possess sizable chemical shift anisotropy, and (iii) its relatively small size allows us to carry out sophisticated quantum chemistry calculations. The molecule under investigation has been assumed to be rigid. Only ring puckering for the saturated cycle could occur. However, as usually assumed for such rings, this possibility has been ruled out.

Solid State NMR. As previously mentioned, solid-state NMR is the primary method used to derive information about CST. Standard experiments were performed in order to access to carbon-13 shielding tensor principal components so as to obtain reference data for subsequent comparison with quantum chemistry calculations and liquid-state determinations. The ND11 was loaded into a 7 mm zirconia rotor, and the ^{13}C NMR experiments were performed at room temperature

(15) Meiboom, G.; Gill, G. *Rev. Sci. Instrum.* **1958**, *29*, 688–691.

(16) Chiarparin, E.; Pelupessy, P.; Ghose, R.; Bodenhausen, G. *J. Am. Chem. Soc.* **1999**, *121*, 6876–6883.

(17) Amato, M. E.; Grassi, A.; Perly, B. *Magn. Reson. Chem.* **1990**, *28*, 779–785.

(18) Tossel, J. A. *Nuclear Magnetic Shieldings and Molecular Structure*; Kluwer Academic: Dordrecht, 1993.

(19) Clark, J. H.; Holland, H. C.; Miller, J. M. *Tetrahedron Lett.* **1976**, *38*, 3361–3364. Bonthron, W.; Cornforth, J. W. *J. Chem. Soc.* **1969**, 1202–1204.

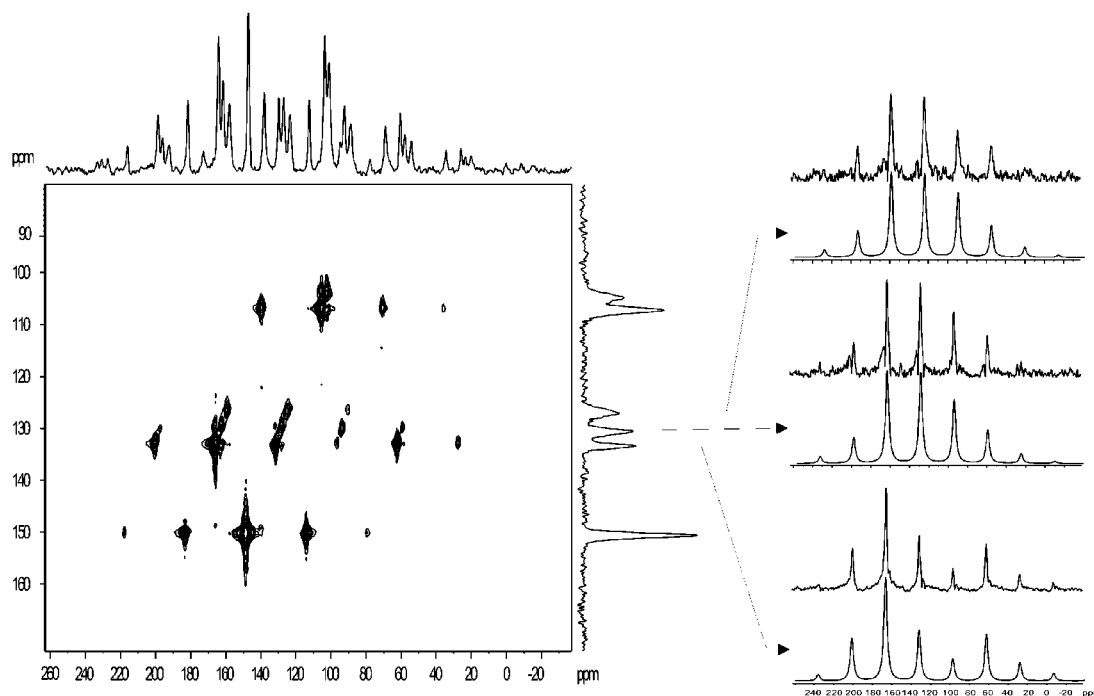


Figure 2. 2D TOSSdeTOSS spectrum used to determine the principal components of the chemical shift tensor for all carbon-13. On the right of the figure are displayed experimental (top) and recalculated (bottom) cross sections corresponding to peaks at isotropic chemical shifts. Experimental parameters were the following: ^{13}C 180° pulse, 8 μs ; spinning frequency, 2600 Hz; recycle time, 240 s; 128 transients.

on a Bruker DSX-300 MHz spectrometer operating at 75.36 MHz. Adamantane served as the external chemical shift standard. The manifold of spinning sidebands resulting from magic angle spinning (MAS, which induces coherent modulation of the CSA) can be exploited so as to extract relevant CST elements. The TOSS experiment²⁰ led to a sideband-free spectrum exhibiting only the isotropic chemical shift. To extract the principal values of the shielding tensor for a given carbon, we have resorted to the two-dimensional TOSSdeTOSS²¹ experiment. Initially, the TOSS subsequence prepares magnetization to yield a period with the sole isotropic shift evolution, while a time-reversed TOSS subsequence restores the anisotropic CSA effect during acquisition. One can then separate the isotropic chemical shift (which is displayed in one dimension) from the shielding anisotropy (displayed in the second dimension). This allows us to extract the corresponding chemical shift anisotropy parameters for each carbon from an appropriate cross section in the 2D spectrum. To check the expected envelope of spinning sidebands, a number of complementary experiments were performed at various spinning speeds. They include standard cross-polarization and dipolar dephasing experiments. The latter led to a simplified spectrum by suppression of signals from protonated carbons. The principal values of the ^{13}C chemical shielding tensor were extracted by fitting the sideband intensities of the 2D TOSSdeTOSS spectra using a homemade program (Figure 2). The sample rotation speeds were set to provide spinning sidebands spanning between four and six orders.

Liquid-State NMR. The ND11 was dissolved in deuterated dimethyl sulfoxide ($\text{DMSO}-d_6$) at a final concentration of 0.5 M. Natural viscosity of $\text{DMSO}-d_6$ slows molecular motions and, as a consequence, decreases the recycle time necessary between consecutive experiments. The sample was carefully degassed by a sequence of “freeze–pump–thaw” cycles, and the tube was subsequently sealed under vacuum. Chemical shifts are referred to TMS. All experiments were carried out at 298 K. Although DMSO presents the advantage of short recycle times, its principal drawback is a viscosity which depends strongly on temperature. As a result, one must take care of the temperature value and stability. Temperature was thus carefully adjusted by means of the

temperature proton chemical shift dependence of methanol,²² the same calibration sample being used for all the spectrometers involved in this study. Cross-relaxation rates were measured on a Bruker Avance spectrometer operating at 9.4 T with an inverse $^1\text{H}/^{13}\text{C}$ probe and using a strategy described elsewhere⁷ which requires 1D and 2D HOESY²³ experiments. Proton decoupling during carbon-13 chemical shift evolution was suppressed in the 2D HOESY experiment in order to access to cross-relaxation rates between chemically equivalent sites in the molecule.²⁴ Because correlation times lie in the picosecond range (extreme narrowing conditions), cross-relaxation rates are field independent, and the experiments have been performed at a single magnetic field value. 1D HOESY experimental parameters are as follows: 64 scans; recycle time, 90 s; 16 mixing times ranging from 0 to 3 s for protonated carbon-13 and from 0 to 20 s for quaternary carbon-13. Identical parameters were used for the two-dimensional experiment with, however, only four mixing times, ranging from 0.1 to 1.0 s. Longitudinal relaxation rates of carbon-13 (T_1) were obtained by means of the inversion–recovery experiment at four different fields: 14.1 (Bruker Avance DRX spectrometer), 9.4 (Bruker Avance DRX spectrometer), 7.03 (Bruker Avance DSX spectrometer), and 5.9 T (Bruker AC spectrometer). Because of the small influence of the carbon CSA relaxation mechanism and of the required accuracy, all T_1 carbon-13 measurements were repeated (at least five times) for each magnetic field value. Inversion–recovery experimental parameters are as follows: 64 scans; 8 dummy scans; 50 s of recycle time; 32 recovery delays ranging from 1 ms to 4 s. Experiments for measuring the $\text{CSA}(\text{C})-d(\text{H}-\text{C})$ cross-correlation rates were performed at 9.4 and 14.1 T using a standard CPMG²⁵ sequence without proton decoupling in such a way that $^1\text{H}-^{13}\text{C}$ couplings are visible in the spectrum. The experimental parameters are as follows: 64 scans; 20 s of recycle time; 5 ms between each 180° pulse; up to 32 mixing times (total duration

(22) Amman, C.; Meier, P.; Merbach, A. E. *J. Magn. Reson.* **1982**, *46*, 319–321.

(23) Yu, C.; Levy, G. C. *J. Am. Chem. Soc.* **1983**, *105*, 6994–6996.

(24) Batta, G.; Kövér, K. E. *Magn. Reson. Chem.* **1988**, *26*, 852–859.

(25) Canet, D.; Mutzenhardt, P. In *Encyclopedia of Analytical Chemistry*; Meyers, R. A., Ed.; John Wiley & Sons Ltd.: Chichester, 2000; pp 12265–12291.

(20) Dixon, T. W. *J. Chem. Phys.* **1982**, *77*, 1800–1807.

(21) Kolbert, A. C.; Griffin, K. G. *Chem. Phys. Lett.* **1990**, *166*, 87.

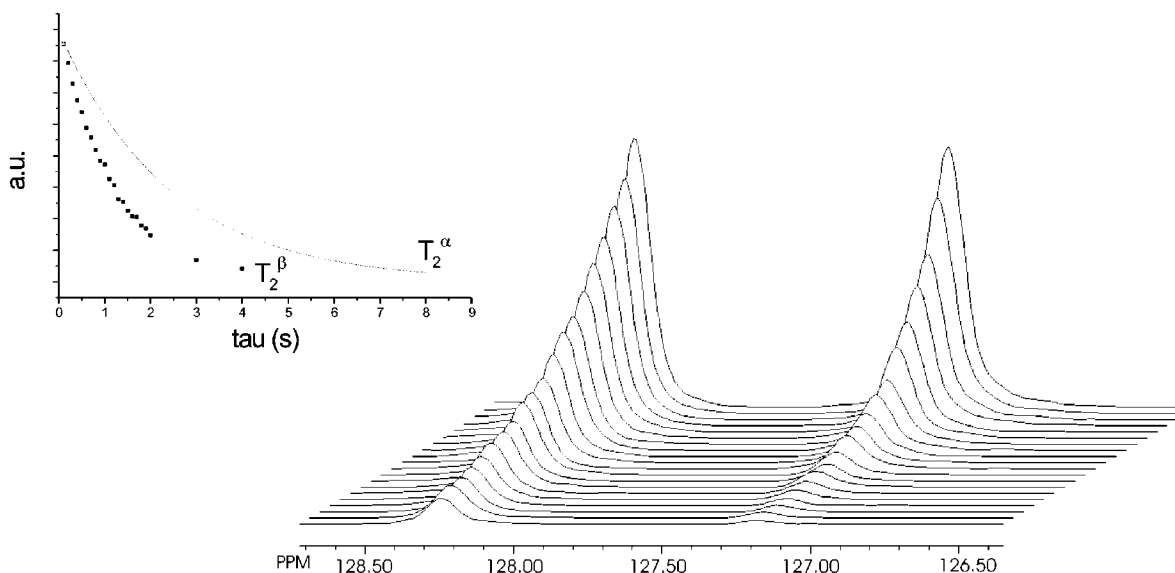


Figure 3. Illustrative decay of the two components in the doublet of a protonated carbon (C5) as observed in the course of the CPMG experiment. The inset shows the corresponding experimental data along with the curves recalculated by the transverse relaxation rates which result from a usual nonlinear fitting procedure.

of the 180° pulse train) ranging from 0.1 to 20 s. For carbon directly bonded to a single proton, each line of the resulting doublet possesses a different transverse relaxation rate (Figure 3), and from this difference the cross-correlation term $\sigma^{d(\text{H}-\text{C}),\text{CSA}(\text{C})}$ can be extracted (see Theory section). To increase the reliability of the carbon-13 data, each experiment was repeated four times.

Quantum Chemistry Calculations

A full interpretation of the experimental data may rely upon ab initio calculations, which yield (i) an optimized geometry of the molecule, (ii) the chemical shielding tensor orientation in the molecular coordinate system, and (iii) the chemical shielding principal components. Because NMR chemical shielding is a very small effect, its calculation requires rather accurate wave functions. As a whole, the Hartree–Fock level of theory neglects the instantaneous interaction between electrons, treating each one in an average or mean field of the others. It happens that in a number of shielding calculations, neglect of electron correlation has serious consequences. Hartree–Fock (at sufficient large basis set) methods give ^{13}C shielding results which are close to experiment for most hydrocarbon molecules and other molecules where electron correlation effects are relatively small. For aromatic compounds, electron correlation²⁶ contributions become more significant, and these effects need to be included in order to obtain accurate shielding tensor prediction. There are basically several ways to go beyond HF theory: Møller–Plesset (MP) or many-body perturbation theory (MBPT), configuration interaction (CI), and density functional theory (DFT). DFT has been shown to be successful in predicting various molecular properties, often giving results of a quality comparable to or even better than those of MP²⁷ for a computational cost of the same order as Hartree–Fock, substantially less than traditional correlation techniques. DFT potentials give accurate results for systems in the ground state and at the equilibrium geometry, in particular when nonlocal electronic density effects are included. However, since many

functionals exist, we tried some combination of exchange (B and B3)^{28,29} and correlation (LYP and PW91)^{30,31} functionals to examine their influence on the chemical shielding tensor. In contrast to the Hartree–Fock based methods, it is not possible to grade the level of theory of these functionals. It is then, a priori, impossible to distinguish which calculation will be the best. Moreover, from the variety of theories available to compute chemical shielding tensors, we decided to adopt the gauge-including atomic orbital (GIAO) method³² for the numerous advantages it presents,³³ and, in addition, methods developed by Keith and Bader, CSGT and IGAIM,³⁴ were considered. It is also well known that the calculated shielding tensor turns out to be very sensitive to basis set size effects and to the geometry employed. To account for these requirements, we decided to retain the 6-311++G** basis set throughout our different calculations. Thus, the working geometry is the one optimized at the B3LYP/6-311++G** level of theory. All calculations were carried out with the Gaussian-98 package.³⁵

Each calculation yields an asymmetric second rank tensor (for each carbon-13) that contains up to nine unique components. Because the antisymmetric contribution of the tensor does not come into the experiment,³⁶ a mathematical treatment of the calculated CST is required corresponding to the transformation described in eqs 2 and 3. Only the symmetric part of the raw calculated tensor was retained; its diagonalization led to its principal components (eigenvalues) and its principal directions

- (28) Becke, A. D. *Phys. Rev. A* **1998**, *38*, 3098–3100.
 (29) Becke, A. D. *Chem. Phys.* **1993**, *98*, 1372–1377.
 (30) Lee, C.; Yang, W.; Parr, R. G. *Phys. Rev. B* **1988**, *37*, 785.
 (31) Perdew, J. P.; Wang, Y. *Phys. Rev. B* **1992**, *45*, 13244–13249.
 (32) Ditchfield, R. *Mol. Phys.* **1974**, *27*, 789.
 (33) Gauss, J. *J. Chem. Phys.* **1993**, *99*, 3629–3643.
 (34) Keith, T. A.; Bader, R. F. W. *Chem. Phys. Lett.* **1992**, *194*, 1–8.
 (35) Frisch, M. J.; Trucks, G. W.; Schlegel, H. B.; Gill, P. M. W.; Johnson, B. G.; Robb, M. A.; Cheeseman, J. R.; Keith, T.; Petersson, G. A.; Montgomery, J. A.; Raghavachari, K.; Al-Laham, M. A.; Zakrzewski, V. G.; Ortiz, J. V.; Foresman, J. B.; Peng, C. Y.; Ayala, P. Y.; Chen, W.; Wong, M. W.; Andres, J. L.; Replogle, E. S.; Gomperts, R.; Martin, R. L.; Fox, D. J.; Binkley, J. S.; Defrees, D. J.; Baker, J.; Stewart, J. P.; Head-Gordon, M.; Gonzalez, C.; Pople, J. A. *Gaussian*; Gaussian Inc.: Pittsburgh, PA, 1995.
 (36) Haeberlen, U. *Advances in Magnetic Resonance*; Academic Press: New York, 1976.

(26) Cybulski, S. M.; Bishop, D. M. *Chem. Phys. Lett.* **1993**, *98*, 8057.

(27) Wiberg, K. B. *J. Comput. Chem.* **1999**, *20*, 1299–1303.

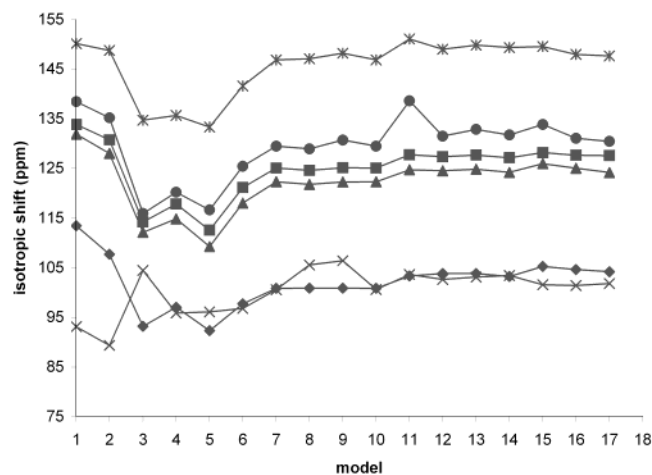


Figure 4. Variation of the isotropic carbon-13 chemical shifts calculated at different levels of theory and basis set. Models from 1 to 15 are respectively GIAO-HF/6-311+G, GIAO-HF/6-311++G**, GIAO-MP2/D95, GIAO-B3PW91/6-31G, GIAO-MP2/6-31G, GIAO-B3LYP/CC-PVDZ, CSGT-B3LYP/6-311++G**, GIAO-BPW91/6-311++G**, GIAO-BLYP/6-311++G**, IGAIM-B3LYP/6-311++G**, GIAO-B3LYP/TZVP, GIAO-B3PW91/6-311++G**, GIAO-B3LYP/6-311++G**, GIAO-B3PW91/CCPVTZ, GIAO-B3LYP/TZV. Models 16 and 17 correspond to the liquid- and solid-state experimental values, respectively. ◆, C3; ■, C5; ▲, C6; ×, C1; *, C2; ●, C4.

(eigenvectors). Finally, because, on one hand, quantum chemistry determines “absolute” displacement or shielding (σ scale), and because, on the other hand, experimental NMR shifts are referenced to some standard (δ chemical shift scale), it was also necessary to compute the chemical shielding σ_{ref} of the reference (TMS), using the same methods and basis sets as for the studied compound. The results obtained using HF, MP2, and DFT theoretical models are compared in order to determine which approach is the more satisfactory. The carbon-13-calculated chemical shift values were computed using mainly the 6-311++G** basis set because it was found to be generally satisfactory for NMR shielding calculations.³⁷ A comparison between calculated and experimental isotropic chemical shifts is presented in Figure 4. It can be seen that the GIAO method with the B3 exchange functional associated with any correlation functional (PW91 or LYP) seems to be the most satisfactory approach, especially when a good enough basis set is used (methods 11–15). This is consistent with the fact that the contribution of the exchange functional is essential, and it shows that B3 is superior to B1. IGAIM and particularly CSGT methods proved to be less accurate in our case. HF and MP2 methods were employed in order to compare their accuracy with that of DFT methods. As previously observed by Wiberg,²⁷ DFT methods give somewhat smaller shielding values (corresponding to larger paramagnetic terms), whereas MP2 gives in most cases significantly larger calculated shielding (corresponding to smaller paramagnetic terms). Also, it has to be mentioned that calculations of chemical shielding parameters at the MP2/6-311++G** level of theory required, for the ND11 molecule, too much disk space to be handled by our computer facilities. MP2 calculations yield the shielding of TMS as 197 ppm, which is considerably larger than both the experimental (186 ppm) and the B3LYP (183 ppm) values. Finally, the GIAO-B3PW91/6-311++G** method (method 12) will be retained, as it yields

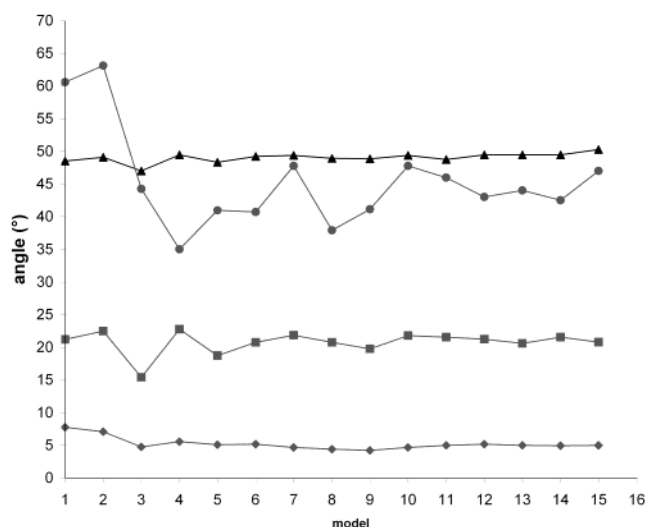


Figure 5. Variation of the angle between the x direction of the chemical shift tensor and the corresponding C–H bond for the same models as in Figure 4 for carbons C2 (▲), C3 (■), C6 (◆), and C4 (●).

the smallest root-mean-square with respect to the experimental carbon-13 chemical shift values in the liquid state. At this point, calculated chemical shielding parameters (orientation and principal components) could be used to evaluate relaxation parameters and thus enable a direct comparison. We turn now to the orientation of carbon-13 CST with respect to the molecular frame. Considering the ND11 molecule and its symmetry properties, it is obvious that CST of carbon-13 involved in the naphthalene ring possesses a principal axis oriented perpendicularly to the ring plane, the two other axes being in the plane. The calculated angle between the CH direction and the x principal direction is displayed in Figure 5. It appears clearly that, whatever method is used, a small variation of only some degrees is observed. The larger variation is observed for the bridgehead carbon C4. For all other carbons, methods labeled 5–15 provide tensor orientation with a deviation which is less than 5°. Conversely, carbon C₄ exhibits a relatively large variation which presumably arises from a particular situation concerning the two principal components in the molecular plane. In that case, the tensor is nearly axial, and it is of importance to be alerted of this situation at the outcome of a quantum chemistry calculation. The two in-plane components differ by only 15–20 ppm (10% of the absolute value), and this quasi-degeneracy explains the variations observed in Figure 5. As a consequence, the contribution of the in-plane orientation of this tensor is negligible (because of its quasi-axiality), and the term $\Delta\sigma_X = \sigma_{xx} - \sigma_{yy}$ tends to zero in the expression of relaxation rates $R_1^{\text{CSA}(C)}$ (eq 12) and $\sigma^{d(H-C),\text{CSA}(C)}$ (eq 14). This ability of a quantum calculation to reproduce the CST orientation at a low level of theory has never been exploited and can be explained by the fact that the CST orientation depends mainly on the molecule’s electronic density, which is already satisfactory at the HF level. The orientation of the chemical shielding tensor is related to the shape of the electronic density around the nucleus. It is obvious that the electronic distribution is mainly directed along the bonds (or orbitals), and even a relatively modest level of calculation represents correctly this shape (and, therefore, the orientation of the chemical shielding tensor). The magnitude of the chemical shielding tensor is related to an accurate description of the value of the electronic density around

(37) Cheesman, J. R.; Trucks, G. W.; Keith, T. A.; Frish, M. J. *J. Chem. Phys.* **1996**, *104*, 5497–5509.

Table 1. Cross-Relaxation Rates Effectively Measured from 1D/2D HOESY Experiments

relaxation vector	$\sigma^{d(H-C)} 5r(s^{-1})$
C_1H_1	0.3590 ± 0.0180
$\text{C}_1\text{H}_1'$	0.3590 ± 0.0180
C_3H_3	0.3879 ± 0.0194
C_5H_5	0.3901 ± 0.0195
C_6H_6	0.4921 ± 0.0246

the nucleus and therefore must be calculated with a high level of theory (i.e., including electronic correlation) and sufficiently large basis set. This observation led us to complement our NMR relaxation data with solely the calculated CST principal directions rather than the corresponding principal components. If we look further at the results listed in Table 6 (below), one may resort to DFT calculations using the gauge-including atomic orbitals. All the functionals used here give comparable results. Furthermore, it appears suitable to use a sufficiently large basis set according to the system under investigation. The triple- ζ valence (TZV) basis set should be considered as possessing minimal capabilities because this set is reasonably accurate for the NMR shielding calculations of first-row atoms and still economical in the case of larger molecules. Moreover, considering a 6-311++G** (two polarization functions and two diffuse functions) basis set increases the accuracy and seems to be the best compromise between accuracy and CPU time. Furthermore, the CC-PVTZ (correlation consistent basis and polarization function included on all atoms) affords somewhat better results with regard to the isotropic chemical shift but increases dramatically the calculation time. Detailed results for all calculations are given in the Supporting Information.

Results and Discussion

Ten cross-relaxation rates could be accurately determined from the whole set of HOESY experiments. These cross-relaxation rates can arise from short-range (carbon directly bonded to proton(s)) or remote (long range) dipolar interactions. So as to deal with accurate experimental data, we decided to retain only short-range cross-relaxation rates (see Table 1), which are anyway more than sufficient for the planned determinations. For the molecule under investigation and from symmetry considerations, we assume that the rotational diffusion tensor and the inertial one coincide. Our assumption is based on the previous work of Huntress,³⁸ who demonstrated the validity of this approach when dealing with a molecule which possesses two planes of symmetry. Nevertheless, a strategy aiming at the determination of the rotational diffusion tensor has been proposed by Dais,³⁹ and more recently Fushman et al. presented a novel approach based on a combination of approximate and exact methods.⁴⁰ In the present case, the five experimental cross-relaxation rates (two of them should lead to identical results because the two relevant vectors are collinear) were fitted against the three correlation times τ_x , τ_y , and τ_z , which are assumed to describe the anisotropic tumbling of the molecule; calculations were made according to eq 15 and to the formulas given in the Supporting Information. The fit was performed using the optimized DFT B3PW91/6-311++G** geometry. This led to the following results, the frame (X, Y, Z)

Table 2. ^{13}C R_1^{CSA} Slopes (See Text) Deduced from Measurements at 5.9, 7.04, 9.4, and 14.1 T and ^{13}C Isotropic Shifts for All Carbons of ND11

carbon	isotropic shift (ppm)	slope $\times 10^4(s^{-1} T^{-2})$
C1	101.94	0.54
C2	147.68	3.30
C3	104.62	3.06
C4	131.00	10.36
C5	127.66	6.14
C6	125.08	7.16

Table 3. CSA Dipolar Cross-Correlation Rates Measured for Carbons C3, C5, and C6 at 9.4 T and 14.1 T^a

carbon	B_0 (T)	$\sigma^{\text{CSA}(C)-d(H-C)}(s^{-1})$	$\sigma/B_0(s^{-1} T^{-1})$
C3	9.4	0.1026	0.011
	14.1	0.1379	0.010
C5	9.4	0.2032	0.022
	14.1	0.2558	0.018
C6	9.4	0.2500	0.027
	14.1	0.3476	0.025

^a The ratio σ/B_0 (right column) demonstrates the consistency of the results.

being defined in Figure 1: $\tau_x = 61.5 \pm 7$ ps, $\tau_y = 42.3 \pm 5$ ps, and $\tau_z = 22.2 \pm 3$ ps, with a rms of $7 \times 10^{-10} s^{-1}$. Because we are using a viscous solvent (DMSO), molecular motions are slowed, and, as a result, correlation times are 2–10 times greater than those obtained in chloroform. As a consequence, this leads to an increase (by similar factors) of all relaxation rates, facilitating their measurement. Nevertheless, molecular motions remain in the extreme narrowing limit, implying that dipolar contributions to relaxation rates are independent of the static magnetic field value. Therefore, if longitudinal relaxation rates exhibit a linear variation according to the square of the magnetic field strength, this reveals the presence of a non-negligible CSA contribution (see eq 12). Experimental slope values (R_1^{CSA} slope) and isotropic shift referenced to TMS are listed in Table 2. The small slope obtained for C1 accounts for the weakness of its chemical shift anisotropy, and its accurate measurement remains a challengingly difficult task. Finally, only CSA(C)– d (H–C) cross-correlation rates involving the one-bond dipolar interactions of monoprotonated carbons (C3, C5, and C6) were successfully measured (Table 3), longer carbon–proton distances or weak chemical shift anisotropy (notably the C1) precluding measurement of this cross-correlation rate for all the other possible carbon–proton pairs. Experiments were performed at the two highest available values of the magnetic field in order to check the validity of the experimental approach. A dedicated program was written in order to fit the CST principal components from these NMR experimental values combined with the quantum calculated tensor orientations (GIAO-B3PW91/6-311++G** method). Table 4 compares C3 principal component values obtained that way with those calculated at all the levels of computation. Similar behaviors were found for C5 and C6 and are supplied in the Supporting Information. It turns out that, whatever the level of theory used in the calculations, our combined approach gives very nicely similar CST principal components (with a dispersion of less than a few parts per million), whereas serious discrepancies can be observed for those calculated solely by quantum chemistry. Our approach, which appears to be reliable and efficient for determining or evaluating the CST of proton-bearing atoms, could be extended to larger molecules for which only a low level of calculations can be

(38) Huntress, W. T. *J. Chem. Phys.* **1968**, *48*, 3524.

(39) Dais, P. *Carbohydr. Res.* **1994**, *263*, 13.

(40) Ghose, R.; Fushman, D.; Cowburn, D. *J. Magn. Reson.* **2001**, *149*, 204.

Table 4. Comparison of the Principal Elements of the Chemical Shift Tensor Obtained for C3^a

model	carbon C3	liquid state				quantum chemistry			
		$\delta_{xx} \pm 5$ ppm	$\delta_{yy} \pm 5$ ppm	$\delta_{zz} \pm 5$ ppm	δ_{iso} (ppm)	δ_{xx}	δ_{yy}	δ_{zz}	δ_{iso} (ppm)
1	GIAO-HF/6-311+G	173.66	117.57	22.63	104.62	198.07	123.12	19.25	113.48
2	GIAO-HF/6-311++G**	174.55	115.68	23.63	104.62	188.41	114.94	19.82	107.72
3	GIAO-MP2/D95	173.67	118.93	21.27	104.62	148.94	102.20	28.47	93.20
4	GIAO-B3PW91/6-31G	174.79	115.16	23.92	104.62	157.57	112.01	21.63	97.07
5	GIAO-MP2/6-31G/6-311++G**	176.4	113.51	23.95	104.62	149.10	102.89	25.06	92.35
6	GIAO-B3LYP/CC-PVDZ	173.39	118.13	22.35	104.62	162.16	108.81	22.18	97.72
7	CSGT-B3LYP/6-311++G**	174.18	116.79	23.19	104.62	166.38	113.50	22.75	100.88
8	GIAO-BPW91/6-311++G**	173.38	118.13	22.34	104.62	164.49	113.39	24.81	100.90
9	GIAO-BLYP/6-311++G**	172.79	119.31	21.75	104.62	165.26	111.89	25.53	100.89
10	IGAIM-B3LYP/6-311++G**	174.08	116.69	23.09	104.62	166.38	113.50	22.75	100.88
11	GIAO-B3LYP/TZVP	173.20	118.51	22.16	104.62	172.00	115.27	22.82	103.36
12	GIAO-B3PW91/6-311++G**	173.73	117.42	22.71	104.62	171.87	116.22	23.45	103.85
13	GIAO-B3LYP/6-311++G**	173.24	118.42	22.20	104.62	172.56	115.06	23.89	103.84
14	GIAO-B3PW91/CC-PVTZ	173.90	117.04	22.90	104.62	170.37	115.71	23.65	103.24
15	GIAO-B3LYP/TZV	174.10	117.13	22.63	104.62	174.22	116.95	24.59	105.25
	min	172.79	113.51	21.27	104.62	148.94	102.20	19.25	92.35
	max	176.40	119.31	23.95	104.62	198.07	123.12	28.47	113.48

^a Liquid state corresponds to CST determined by combining NMR relaxation data with the CST orientation obtained by quantum chemistry calculations. One can notice the greater difference between minimum and maximum values of the principal elements obtained from quantum chemistry alone.

Table 5. Experimental versus Calculated R_1^{CSA} Slope (See Table 2) for Carbons C1, C2, and C4

carbon	experimental $\times 10^4$ ($\text{s}^{-1} \text{T}^{-2}$)	calculated $\times 10^4$ ($\text{s}^{-1} \text{T}^{-2}$)
C1	0.54	0.57
C2	3.30	2.87
C4	10.36	8.85

Table 6. Chemical Shift Principal Components of Carbon-13 in the ND11 Molecule^a

		ppm			
		δ_{xx}	δ_{yy}	δ_{zz}	δ_{iso}
C1	solid state	128.53 \pm 1	103.34 \pm 1	74.52 \pm 1	102.13
	quantum chemistry	136.67	102.54	68.71	102.64
C2	solid state	217.14 \pm 1	142.56 \pm 1	83.82 \pm 1	147.84
	quantum chemistry	217.21	145.24	84.61	149.02
C3	liquid state	173.73 \pm 5	117.42 \pm 5	22.71 \pm 5	104.62
	solid state	168.18 \pm 1	119.21 \pm 1	26.00 \pm 1	104.46
C4	quantum chemistry	171.87	116.22	23.45	103.85
	solid state	204.50 \pm 1	187.93 \pm 1	-1.17 \pm 1	130.42
C5	quantum chemistry	205.60	191.46	-2.56	131.50
	liquid state	235.86 \pm 5	132.53 \pm 5	14.59 \pm 5	127.66
C6	solid state	223 \pm 1	140.42 \pm 1	20.06 \pm 1	127.83
	quantum chemistry	229.48	131.88	20.74	127.37
C6	liquid state	220.71 \pm 5	145.62 \pm 5	8.62 \pm 5	125.08
	solid state	226 \pm 1	135.77 \pm 1	10.87 \pm 1	124.21
	quantum chemistry	232.35	134.81	6.50	124.55

^a Solid state row: data deduced from solid-state NMR experiments. Liquid state row: data determined by a combination of liquid-state NMR relaxation experiments and quantum chemistry calculations (see text). Quantum chemistry row: calculated at the GIAO-B3PW91/6-311++G** level of theory.

considered. As previously mentioned, C1 exhibits a too weak anisotropy which prevents any CST determination; moreover, it was not possible to measure the CSA(C)- d (H-C) cross-correlation rates for C2 and C4, and, in that case, we can simply compare experimental and calculated R_1^{CSA} slopes. Table 5 shows a fairly good agreement between experimental and recalculated values, which demonstrates that calculated CST orientations and magnitudes constitute, at least, a correct estimate. Solid-state experiments yield CST principal components for all the carbons in the molecule. Table 6 gives an overall view of the results obtained in this work with tensor orientations displayed in Figure 1. None of the CST shows a particular symmetry (even if the CST of C4 is close to an axial symmetry).

Chemical shift principal components determined by our combined approach (C3, C5, and C6) are in a very good agreement with those measured through solid-state experiments. Indeed, no appreciable variation of the carbon-13 CST was expected between the solid phase and the liquid phase for the ND11 molecule. Nevertheless, several small deviations (a maximum of 13 ppm for δ_{xx} of carbon C5, 5.5% of the absolute value) are noticed. They may arise from experimental uncertainties or from the intrinsic difference between the two physical states; due to the smallness of these deviations, it would be illusory to pursue this discussion. Quantum chemistry and solid-state results also show a very good agreement for all the carbons in the molecule; once again, DFT proved to be a powerful technique for computing chemical shift tensors.²⁷

Concerning the chemical shift orientation, the lower component denoted by δ_{zz} is perpendicular to the molecular plane; such a situation is generally observed in molecules with reflection plane (containing the naphthalene moiety) symmetry⁴¹ and arise from ring currents that lie in the molecular plane.⁴² These currents produce a secondary magnetic field which reinforces the external magnetic field in the region of the considered carbon nuclei, causing a paramagnetic (i.e., down-field) shift. The in-plane component, δ_{yy} , is the one that arises from a paramagnetic current involving the π electrons of two adjacent C-C bonds, whereas the other in-plane component, δ_{xx} , lies nearly along the C-H bond⁴³ (C3, C5, and C6) and therefore depends on the π electron contribution but also on a contribution from the σ electrons of the two adjacent CC bonds. In Figure 1, the Mayer⁴⁴ bond orders calculated at the B3PW91/6-311++G** level of theory are shown for ND11. The deviation of the δ_{xx} axis from the C-H direction can be rationalized in terms of the Mayer bond order of the adjacent C-C bond. The δ_{xx} axis tends to orient along the direction which is perpendicular to the bond with the largest π character, or, in other words, the largest bond order. It is observed that the

- (41) Sherwood, M. H.; Facelli, J. C.; Alderman, D. W.; Grant, D. M. *J. Am. Chem. Soc.* **1991**, *113*, 750–753. Carter, C. M.; Alderman, J. C.; Facelli, J. C.; Grant, D. M. *J. Am. Chem. Soc.* **1987**, *109*, 2639–2644. Barich, D. H.; Facelli, J. C.; Hu, J. Z.; Alderman, D. W.; Wang, W.; Pugmire, R. J.; Grant, D. M. *J. Am. Chem. Soc.* **2001**, *39*, 115–121.
(42) Lazzaretti, P. *Prog. NMR Spectrosc.* **2000**, *36*, 1–88.
(43) Facelli, J. C.; Grant, D. M. *Theor. Chim. Acta* **1987**, *71*, 277–288.
(44) Mayer, I. *Chem. Phys. Lett.* **1982**, *97*, 270–273.

deviation of δ_{xx} from the C–H direction increases as one moves from the terminal ring to the five-membered ring. The corresponding differences between the calculated bond orders of the two adjacent C–C bonds also show a similar trend. As a general rule for bridgehead carbons and in the case where all three bonds exhibit different bond orders, the δ_{xx} component strikes a compromise between being parallel to the bond with the lowest bond order and being perpendicular to the bond with the highest bond order. C2 and C4 chemical shift tensors obey these rules, as shown in Figure 1.

Conclusion

Determination of the CST in the liquid state is certainly a challenging task. It requires the characterization of molecular tumbling, by using either analytical spectral densities (for small or medium size molecules) or spectral density mapping⁴⁵ (in the case of large biomolecules), as done recently by Graslünd and co-workers.⁴⁶ If no assumption can be made about the symmetry of CST, the lack of relevant observables (dependent on CST) precludes their full determination. We have shown in this paper that this issue can be efficiently solved by combining NMR relaxation data with only one piece of information provided by quantum chemistry calculations, namely the tensor orientation. This approach proves to be feasible in numerous situations, because this orientation can be satisfactorily computed without resorting to state-of-the-art calculations. Consistent chemical shift tensors have been determined for only some carbons in the molecule under investigation, whatever the level of computation used. Nevertheless, two major limitations prevent the determination of CST in the general case. First, carbons must have a sizable chemical shift anisotropy, and second, without isotope labeling, carbons must be bonded to proton(s) so as to measure additional relaxation parameters, for instance, cross-correlation rates. Previous studies on proteins have demonstrated the possibility to determine the magnitude of ^{15}N CSA from the field dependence of autorelaxation rates and ^1H – ^{15}N NOE measurements, complemented^{47,48} or not^{49,50} by

measurement of cross-correlation rates between the ^1H – ^{15}N dipolar interaction and ^{15}N CSA. An elegant method called the “model-independent” approach was recently suggested^{51,52} which is based on the analysis of R_2 and cross-correlation rates. Extension of our methodology outside the extreme narrowing limit (i.e., for larger molecule such as proteins) is also possible for both carbon-13 and nitrogen-15 nuclei. This can be presently envisaged because (i) molecular dynamics can be characterized by an appropriate set of relaxation parameters measured at different values of the magnetic field, and (ii) local quantum chemistry calculations are possible using, for instance, a QM/MM strategy⁵³ like the ONIOM^{54,55,56} approach, which subdivides a molecule into several parts of layers, each being described at a different level of theory. An alternative to QM/MM consists of isolating the local environment around a nucleus.⁵⁷ Quantum chemistry determination of the chemical shielding orientation could be included in these calculations with reasonable sizes of both the basis set and the theoretical level (as demonstrated in the present work) and with a minimum of penalty regarding computational time. The main issue in these systems comes from the fact that, outside the extreme narrowing limit, all relaxation rates become field dependent, and, therefore, the separation between the dipolar and CSA contributions in some relaxation rates will be more difficult.

Acknowledgment. We are most grateful to the “Service Commun de Biophysicochimie des Interactions Moléculaires”, directed by the Prof. G. Branlant (Université Henri Poincaré, Nancy 1), for the use of their 14.1 T Bruker Avance spectrometer. We are also grateful to IDRIS center which provides us CPU time for quantum calculations. Dr. X. Assfeld is acknowledged for helpful discussions on quantum chemistry, and Dr. J. P. Joly is acknowledged for molecule synthesis.

Supporting Information Available: Hubbard’s equations and tables of NMR data (PDF). This material is available free of charge via the Internet at <http://pubs.acs.org>.

JA0166702

(45) Peng, J. W.; Wagner, G. *Biochemistry* **1992**, *31*, 8571–8586.

(46) Damberg, P.; Jarvet, J.; Allard, P.; Graslünd, A. *J. Biol. NMR* **1999**, *15*, 27–37.

(47) Kroenke, C. D.; Rance, M.; Palmer, A. G. *J. Am. Chem. Soc.* **1999**, *121*, 10119.

(48) Tjandra, N.; Szabo, A.; Bax, A. *J. Am. Chem. Soc.* **1996**, *118*, 6986.

(49) Fushman, D.; Tjandra, N.; Cowburn, D. *J. Am. Chem. Soc.* **1999**, *121*, 8577.

(50) Canet, D.; Barthe, P.; Mutzenhardt, P.; Roumestand, C. *J. Am. Chem. Soc.* **2001**, *123*, 4567.

(51) Fushman, D.; Cowburn, D. *J. Am. Chem. Soc.* **1998**, *120*, 7109.

(52) Fushman, D.; Tjandra, N.; Cowburn, D. *J. Am. Chem. Soc.* **1998**, *120*, 10947.

(53) Murphy, R. B.; Philipp, D. M.; Friesner, R. A. *J. Chem. Phys.* **2000**, *113*, 5604–5613.

(54) Karadakov, P. B.; Morokuma, K. *Chem. Phys. Lett.* **2000**, *317*, 589.

(55) Svensson, M.; Humbel, S.; Froese, R. D. J.; Matsubara, T.; Sieber, S.; Morokuma, K. *J. Phys. Chem.* **1996**, *100*, 19357.

(56) Humbel, S.; Sieber, S.; Morokuma, K. *J. Chem. Phys.* **1996**, *105*, 1959.

(57) Scheurer, C.; Skrynnikov, N. R.; Lienin, S. F.; Strauss, S. K.; Brüschweiler, R.; Ernst, R. R. *J. Am. Chem. Soc.* **1999**, *121*, 4242.